Monte Carlo simulation of converging laser beams propagating in biological materials

Zhi Song, Ke Dong, Xin H. Hu, and Jun Q. Lu

A new method of Monte Carlo simulation has been developed to simulate the spatial distribution of photon density of converging laser beams propagating in a turbid medium such as the phantom of biological tissue. This method can be used to obtain steady-state light distribution in the tissue phantom for a continuous-wave laser beam. We have calculated the steady-state distribution of the photon density and found important features that are uniquely related to the propagation of the converging beams in the tissue phantom. © 1999 Optical Society of America

OCIS codes: 000.4430, 170.6930, 290.4210.

1. Introduction

Generally, precise modeling of the propagation of light in turbid media such as the biological tissues has remained as a fundamental challenge. Investigation of light propagation in these materials requires that both the absorption and the scattering of the light be considered. Among different approaches, the radiative transport theory[1] has served as the foundation for many theoretical investigations. In this approach, the radiation field of light is analyzed in terms of the radiance on the basis of energy conservation, and the light interaction with the medium is described through absorption and scattering processes. Except for only a few cases of simple geometry for which analytical solutions can be obtained, various approximations and numerical methods have been used to solve the radiative transfer problems with practical boundary conditions. On the other hand, the principle of the radiative transfer theory can be equally served by use of statistical methods in which the light distribution is treated as a collection of classical particles, i.e., the photons with no direct characterizations of phase and polarization. The interaction of the photons with a turbid medium can then be studied with a random-walk model of Monte Carlo simulation. Over the past decade, the Monte Carlo simulation has been given considerable attention in the studies of interaction between visible or near-infrared light and the turbid media of the biological tissues.[2–6] This is mostly because of its potential to offer nearly exact solutions for three-dimensional (3-D) problems of light propagation based on the radiative transfer theory with virtually any boundary conditions. Therefore it has significant advantages over approximate methods such as the diffusion approximation of the radiative transport equation[7] and the more approximate Kubelka–Munk two-flux theory[8] in obtaining a complete understanding of light distribution. In the past, the heavy demand of computation time of the Monte Carlo simulation to reduce statistical errors has impeded wide application of the method. With the recent advent of low-cost personal computers with high computation power, it appears that the potential of Monte Carlo method can now be fully appreciated.

Solution of a general problem of radiation dosimetry in biological materials yields two distinctly different types of results. The first result provides the spatial distribution of energy deposition of the radiation in the medium due to absorption; it is often needed in cases such as the modeling of photodynamic therapy. The second result furnishes the spatial distribution of the radiation energy, inside or through the tissue, which supplies important information on the availability of radiation for either diagnostic or therapeutic purposes.

Previous Monte Carlo simulations of the light–tissue interaction have mainly provided the first type of results either in steady-state form for cw laser

The authors are with the Department of Physics, East Carolina University, Greenville, North Carolina 27858. Z. Song is on leave from the Department of Physics, Nankai University, Tianjin 300071, China.

Received 28 September 1998; revised manuscript received 15 January 1999.

0003-6935/99/132944-06$15.00/0

beams[2–5] or in time-resolved form for short-pulsed beams.[6] In these studies a method of spatial impulse convolution has been used to achieve a significant reduction in computation time.[3,5,6] For this, only collimated laser beams of finite diameters are considered, since all the elements in a beam must have the same direction when incident on a boundary of a tissue sample. The paths of photons injected through a single point at the air–medium interface are first followed individually until all photons are absorbed by or escape from the interested region and the corresponding spatial distribution of absorption events is recorded. Then the spatial distribution of absorbed light energy is obtained without further simulation by use of convolution integration for the collimated beam of arbitrary shape in which all the elements in the beam have the same direction at the air–medium interface. The high computational efficiency of the above method disappears, however, if used to simulate a converging laser beam incident on the tissue, because the boundary condition varies for beam elements at different locations.

In this paper, we report a new method of Monte Carlo simulation that provides an efficient and direct solution to spatial distribution of light within tissue for the second type of the radiation dosimetry problems. Although the light distribution within the tissue is examined here only for converging beams, this method can be applied to systems with arbitrary boundary conditions and arbitrary forms of incident beam in either steady-state or time-resolved forms. Furthermore, the new method can be used to simulate the effect of rough surfaces on the light propagation in the turbid media. In Section 2 we give a detailed description of the method. The steady-state results on the propagation of an initially focused laser beam in tissue phantoms and a discussion of their dependence on beam profiles and optical parameters of the tissue are presented in Section 3, followed by a summary in Section 4.

2. Methodology

We consider a cylindrically symmetric problem in which a focused, monochromatic laser beam is incident on a tissue phantom from air at time t_0 with the central axis of the beam coinciding with the z axis. The tissue is assumed to be macroscopically homogeneous and to occupy the half space of $z \geq 0$ with a finite region considered in the simulation. It is characterized by an index of refraction n, scattering coefficient μ_s, asymmetry factor g, and absorption coefficient μ_a. For simplicity, we assume that the air–tissue boundary is optically planar and smooth and that it overlaps with the x–y plane ($z = 0$). The beam's initial configuration at t_0 is described by two parameters defined inside the tissue, the cone angle α and the distance d between its geometric focal point and the air–tissue boundary, as shown in Fig. 1. We assume that all photons are injected on the tissue side of the boundary: $z = 0^+$. The angle with respect to the z axis, at which a photon starts to propagate, is a function of the photon's distance ρ[equal to $(x^2 + y^2)^{1/2}$] at the $z = 0$ plane according to specific beam profile and cone angle. To track the 3-D trajectories of photons contained in an incident beam, we have adopted a scheme similar to those previously used.[2,3]

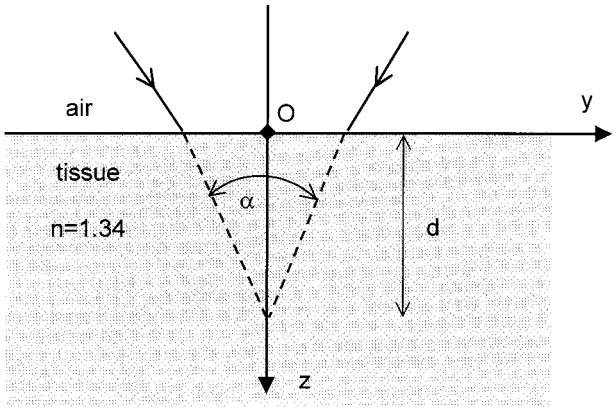

Fig. 1. Geometric configuration of a converging laser beam incident on a phantom of the biological tissue from air where $\alpha = 30°$, $d = 1.0$ mm, and the refractive index of the tissue $n = 1.34$.

The boundary condition for each photon contained in the beam is first set according to its distance ρ from the z axis and the given beam parameters. Before a photon is released, its lifetime, τ, is randomly chosen from an exponential distribution function with an average value $\langle\tau\rangle = 1/(v\mu_a)$, where μ_a is the absorption coefficient of the tissue and v is the light speed in the tissue. Therefore the total travel distance is predetermined to be $L_a = v\tau$. The photon then starts to propagate inside the tissue until scattered. The travel distance L_s between successive scattering events is again randomly chosen from an exponential distribution function with an average value $\langle L_s\rangle = 1/\mu_s$, where μ_s is the scattering coefficient of the tissue. The new propagation direction of the photon in the 3-D space after the scattering is determined by two angles, θ and ϕ, with respect to the incident direction of the photon before scattering. The scattering angle θ is the angle between the incident and the scattered directions governed by the Henyey–Greenstein distribution function[9] and is needed to satisfy $\langle\cos\theta\rangle = g$.[10] The azimuthal angle ϕ is randomly chosen to determine the projection of the new direction in the plane perpendicular to the incident direction. Before the photon is allowed to propagate further after a scattering event, the total distance L traversed by the photon along its trajectory is calculated to test if it exceeds the predetermined L_a. If $L \geq L_a$, the photon is then eliminated as a result of absorption. Otherwise, the photon's position is further checked to determine if it is on the boundaries of the considered region in the tissue. When the photon is on the air–tissue boundary, it is either reflected back into the tissue, with a probability equal to the Fresnel reflection coefficient, or eliminated for its escape into the air. The photon is also eliminated if it travels beyond the other boundaries of the considered

region. If the photon survives these tests, it is allowed to propagate further until one of the eliminating conditions discussed above is met. The procedures are repeated until all the photons contained in the beam are depleted.

To record directly the spatial distribution of photon density inside the tissue, we have developed a time-slicing method based on the temporal recording of each photon's trajectory after its initial injection at the time t_0. This method has the benefits of calculating both transient and steady-state distributions of light and the high computational efficiency for converging beams. In this method, we first consider a monochromatic laser beam of only one temporal impulse containing N_0 photons,

$$N_0 F(\rho)\delta(t - t_0)\delta(z = 0_+),$$

where $N_0F(\rho)$ provides the beam profile in terms of surface density of photon at the air–tissue boundary. The initial direction of an injected photon is obtained by backprojection to the $z = 0$ plane from a spherical wave front of radius d centered at the focal point located on the z axis at $z = \mathrm{d}$, which is allowed for the steady-state calculation within the radiative transfer framework. The considered region of the tissue is divided into a grid of cubic cells of volume b^3 with each side parallel to the x, y, and z axes. Using the scheme described above, we recorded the position of each tracked photon in the impulse along its 3-D trajectory inside the tissue according to which cell the photon traverses at time t_i ($i = 1, 2, \ldots m$). This sequence of time, $t_{i+1} > t_i > t_0$, separates the temporal course of the tracked photon during its lifetime into many small and equal segments that are called the time slices. Each time slice has the same duration of

$$\Delta t_0 = t_{i+1} - t_i = \frac{a}{v},$$

where a is the travel distance of the photon that is chosen to be smaller than b and much smaller than $\langle L_s \rangle$. For the results reported in this paper, we used $\Delta t_0 = 4.47fs$ or $a = 1.00\ \mu\mathrm{m}$, $b = 2.00\ \mu\mathrm{m}$, and $n = 1.34$. The maximum slice number, $m_{\max}$, among all of the tracked photons is defined to be the m of the photon that lasts the longest. Therefore $m_{\max}$ varies slightly owing to the random nature of the maximum lifetime τ of the tracked photons among different simulations with identical parameters. After all, the N_0 photons in the temporal impulse are tracked, and the photon density per unit time at time t_i can be obtained by one's tallying the number of photons that traverse through the jth cell during Δt, denoted as

$$\frac{W_j(t_i)}{b^3 \Delta t},$$

where Δt is the dwelling time of a photon inside a cell averaged over all N_0 photons and $W_j(t_i)$ is the number of photons in jth cell at time t_i. The function

$$\frac{W_j(t_i)}{b^3 \Delta t}$$

then provides the time evolution of the photon density per unit of time at the location of jth cell as a consequence of the initial injection given by $N_0F(\rho)\delta(t - t_0)\delta(z = 0_+)$. It is straightforward to obtain light distributions in time-resolved forms from the set of the functions $\{W_j(t_i)\}$.

The information embodied in $\{W_j(t_i)\}$ can be organized in the following fashion so that steady-state distributions of the photon density for a laser beam of arbitrary spatial profiles at the tissue boundary can be obtained efficiently. To illustrate this point, we consider a case of square pulse of finite duration t_p containing N photons with initial injection occurring at $t = t_0$. This problem can be conceived as the numerical equivalent of the superposition of m' identical temporal impulses over the pulse duration separated by Δt_0 with the requirement that $\Delta t_0 \ll t_p$. If each impulse contains N_0 photons, we must have

$$N = N_0 \times m'$$

with $N\hbar\omega/t_p$ corresponding to the peak power of the incident beam at $z = 0_+$, where $\hbar\omega$ is the photon energy. The condition for a sufficiently long pulse to establish a steady-state distribution of light is furnished by requiring that $m' \geq m_{\max}$. The parameters $m_{\max}$ and Δt_0 have been defined in the above discussion of the single-impulse case. The steady-state distribution of light, achieved after $m_{\max}\Delta t_0$ and well before the end of the pulse, can be calculated as the photon density during the dwelling time Δt in the jth cell with the following time summation:

$$\frac{W_j}{b^3} = \sum_{i=0}^{m_{\max}} \frac{W_j(t_i)}{b^3}.$$

Obviously, the simulation of steady-state distributions demands much less computer memory than the time-resolved simulations for not keeping the middle results $\{W_j(t_i)\}$ during the photon tracking.

3. Numerical Results

Using the new time-slicing method, we have simulated the steady-state distribution of photon density for a tightly focused laser beam inside a phantom modeling the biological tissues, as shown in Fig. 1. The cone angle of the focused beam was set to $\alpha = 30°$, and the focused point was located at $d = 1.0$ mm away from the air–tissue boundary. The wavelength of the light was assumed to be approximately 1 μm and the refraction index of the tissue to be $n = 1.34$ for the tissue phantom. For the spectral region of near infrared, it is well known that scattering dominates the light–tissue interaction for most soft tissues and is peaked strongly in the forward direction. As a result, the asymmetric factor of scattering $g =$

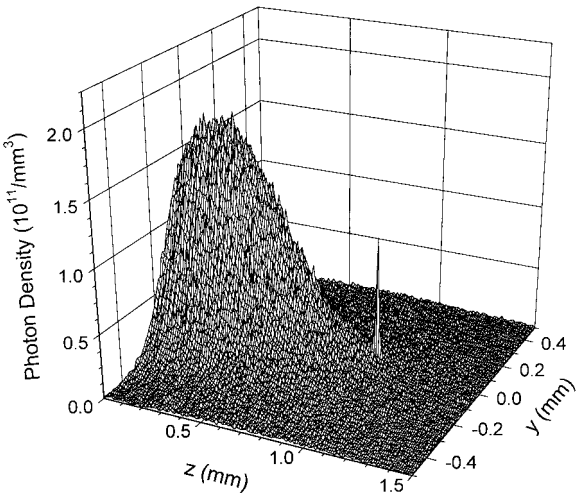

Fig. 2. Steady-state distribution of photon density in the y–z plane of the tissue for a converging incident laser beam. The profile of the incident laser beam at the air–tissue boundary is Gaussian with a radius $r = 0.268$ mm defined at $(1/e^2)$ of the central peak. Parameters for the tissue are $\mu_s = 10.0$ (mm^{-1}), $\mu_a = 0.5$ (mm^{-1}), and $g = 0.9$.

$\langle \cos\theta \rangle$ was chosen to be 0.9.[11] However, the experimental determination of optical parameters, μ_s and μ_a, in the near-infrared region has been scarce and results vary significantly, for example, for the skin tissues.[5,8,10] Two values of μ_s and two beam profiles of $F(\rho)$ have been used in our simulations to investigate the dependence of the light propagation on these parameters. For results presented in this paper, we chose $\mu_s = 10$ (mm^{-1}) or 5 (mm^{-1}) and $\mu_a = 0.5$ (mm^{-1}) and limited our photon tracking in a considered region of the tissue with -0.5 mm $\leq x$ (or y) ≤ 0.5 mm and $0 \leq z \leq 1.5$ mm unless otherwise specified. The size of the considered region is chosen to be large enough so that the effect of the returning photons from outside of the region is negligible on presented results.

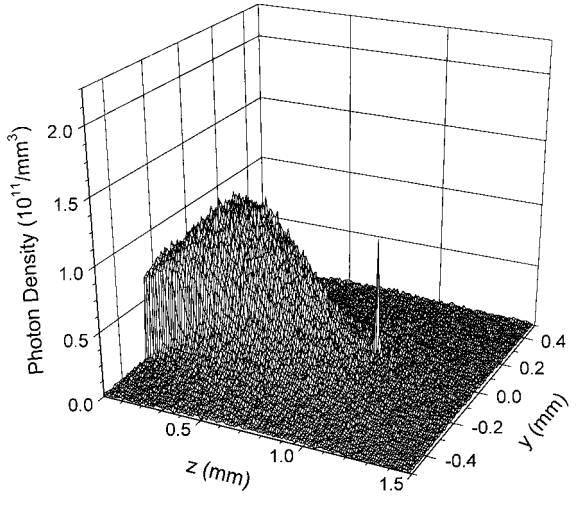

Fig. 3. Same as Fig. 2, except for a laser beam of top-hat profile with the same radius $r = 0.268$ mm.

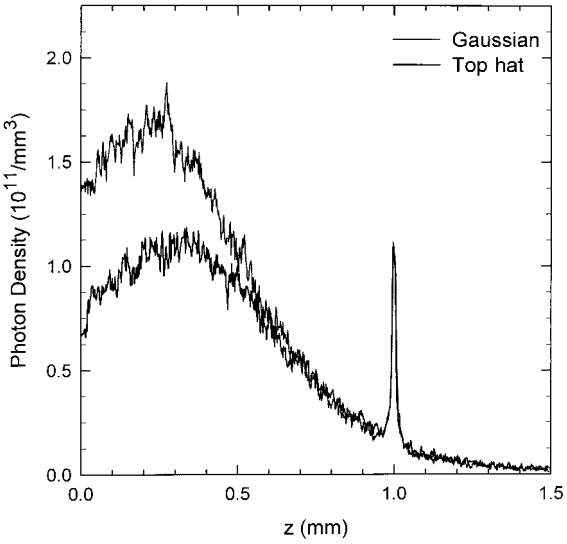

Fig. 4. Comparison of the photon density on the z axis for the two cases shown in Figs. 2 and 3.

In Fig. 2 we present the photon-density distribution in a cross section of the tissue containing the y and the z axes for a focused incident beam of Gaussian profile. The e^{-2} radius of the incident beam is 0.268 mm at the boundary $z = 0_+$, and the total number of the tracked photons is $N_0 = 1.41 \times 10^7$. A maximum slice number of $m_{\max} = 7438$ is found in this simulation to obtain a steady-state distribution. The number of scattering events experienced by individual photon ranges from 0 to 77 with a mean of 10. Figure 2 shows that the photon density along the beam center initially increases as the beam starts to penetrate into the tissue because the initially focused laser beam remains partially converging. For $z > 0.3$ mm, the density starts to decrease and is gradually defocused owing to the scattering. Nevertheless, a well-defined peak is observed at the geometric focal point relative to the background formed by the scattered photons. Obviously, this peak consists mostly of the very few photons that have arrived at the focal point of the incident focused beam before their first scattering event. According to Fig. 2, for a steady-state light distribution with a photon supply of $N_0 = 1.41 \times 10^7$ per unit time, we observe approximately a total of 363 photons per unit time arriving in the cell at the focal point without scattering. This agrees well with the number of unattenuated photons reaching the focal point, 387, predicted by the radiative transfer theory. Unattenuated photons could exist in turbid media beyond the penetration depth $1/(\mu_a + \mu_s)$, but only converging beams can gather them together. At depths that are not too large in comparison to $1/(\mu_a + \mu_s)$, the unattenuated photons from a converging laser beam have a density significantly higher than the background of scattered photons. Currently, we are investigating potential applications based on this unique nature of converg-

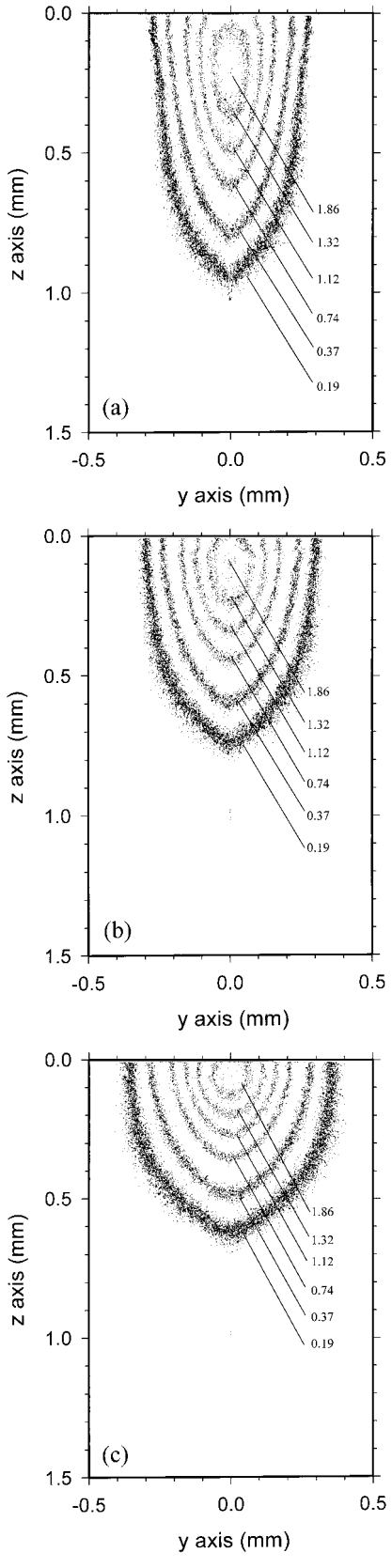

Fig. 5. Dependence of photon density on the asymmetry parameter g: (a) contour diagram of Fig. 2 where $g = 0.9$; (b) same as part (a), except $g = 0.8$; (c) same as part (a), except $g = 0.6$. The photon density of each contour is indicated by the attached number with a standard deviation of ± 0.3 in the unit of $(10^{11}/\text{mm}^3)$.

ing laser beams propagating in a turbid medium, and the results will be reported elsewhere.

A converging beam of top-hat profile at the air–tissue boundary was simulated to study the effect of boundary conditions on light distribution inside the tissue. The top hat refers to a transverse profile for a laser beam that has a uniform irradiance within the beam diameter and the irradiance becomes zero outside the diameter. Figure 3 shows the photon-density distribution in a cross section of the tissue containing the y and the z axes for the top-hat beam of the same radius as the Gaussian beam displayed in Fig. 2. Here the total number of photons is $N_0 = 1.39 \times 10^7$, and the number of scattering events for individual photons ranges from 0 to 96 with a mean of 10. The maximum slice number is $m_{\max} = 9360$. Although the difference between $m_{\max}$ of the Gaussian and the top-hat beams appears significant, note that the mean values of the slice number are nearly the same between the two simulations. Comparing Fig. 3 with Fig. 2, we can recognize that the difference in the two distributions is mostly prominent near the air–tissue boundary. For both cases, the maxima of the photon-density distributions occur on the beam center inside the tissue, with the top-hat beam's maximum penetrating slightly deeper. This is clearly demonstrated in Fig. 4 in which the photon density is plotted as a function of depth on the z axis for the converging beams. For direct comparison, the curve for top-hat beam is scaled to the same number of incident photons as the Gaussian beam.

The influence of the asymmetric factor of scattering, g, on the light propagation in tissue was also studied with two additional values of g, 0.8 and 0.6. For these additional values to be compared with the result in Fig. 2, where $g = 0.9$, light distributions of identical Gaussian beams in tissues having different g are depicted in Fig. 5 with photon-density contours in the y–z plane. For Fig. 5(c) with a small value of g ($=0.6$), a larger considered region [-1.5 mm $\leq x$ (or y) ≤ 1.5 mm and $0 \leq z \leq 3$ mm] was used to reduce the effect of the returning photons from outside of the considered region on the contour near boundaries. It is clearly seen that as g decreases from 0.9 to 0.6, the penetration capability of the converging beam decreases rapidly and the diffusion of the beam in the transverse direction becomes pronounced. For quantitative comparison, the photon densities of the three cases are plotted as a function of depth on the z axis in Fig. 6. As for the peak at the focal point, the height of the peak relative to the diffusive background is almost the same for all the three cases, but the background around it increases with g for increasing scattering in the forward direction.

The change in scattering coefficient of the tissue, μ_s, can result in a drastic difference in the focusing capability of a laser beam inside the tissue because of the exponential dependence of the unattenuated photon at the focus on μ_s. Replacing $\mu_s = 10\ (\text{mm}^{-1})$ in Fig. 2 by $\mu_s = 5.0\ (\text{mm}^{-1})$, we can see a steep increase in the number of photons arriving at the focal point, as shown in Fig. 7. This indicates that accurate knowledge of

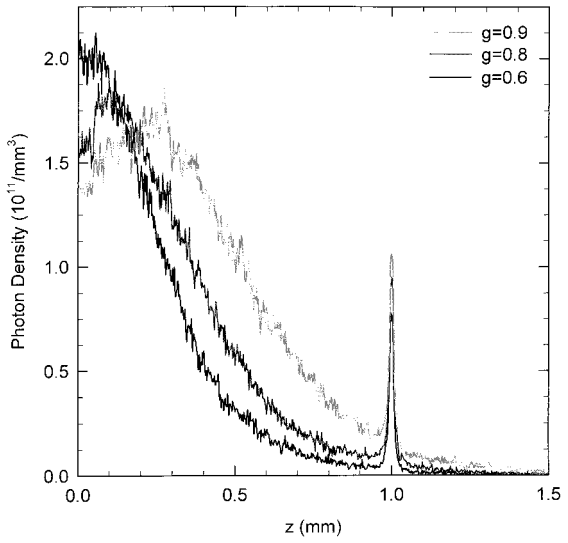

Fig. 6. Comparison of the photon density on the z axis for the three cases shown in Fig. 5.

the scattering coefficient of a turbid medium is needed if a focused laser beam inside the turbid medium is desired. One example of potential applications is to scan a focused laser beam of nanosecond pulses for treating pigmented lesions in skin dermis.[12]

On the other hand, the separate dependence of the light distribution near the focus on μ_s and g points to the fact that our results are quite different from those calculations based on the diffusion approximation. According to the diffusion approximation for cases where $\mu_s' \gg \mu_a$, the diffusion coefficient of the migration photons depends only on the reduced scattering coefficient $\mu_s' = \mu_s(1 - g)$.[13] The difference observed here is because the majority of the photons near the focus point are nondiffusive. It thus shows that the diffusion approximation is not valid for the cases we considered in this paper, even though the scattering dominates the light interaction with the medium.

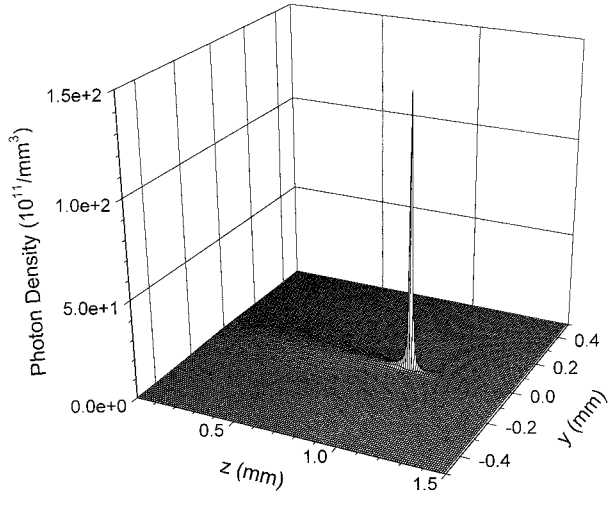

Fig. 7. Same as Fig. 2, except $\mu_s = 5.0$ (mm^{-1}).

4. Summary

We have developed an efficient method of Monte Carlo simulation to investigate the propagation of converging laser beams in biological tissues numerically. Because of this method, we can directly obtain the steady-state distributions of photon density of a laser beam in a macroscopically homogeneous tissue phantom for nearly any beam configuration and tissue geometry. The simulation of steady-state distribution of photon density has revealed several new features concerning the propagation of converging laser beams in the turbid media of tissues. Further experiments on testing these simulation results are in progress.

Program development and testing were completed on personal computers purchased with internal grants from East Carolina University. Numerical simulations were performed on the Cray T90 supercomputer through a grant from the North Carolina Supercomputing Center. X. Hu acknowledges the partial support through a research grant from the National Institute of Health (R15GM/OD55940-01).

References

1. S. Chandrasekhar, *Radiative Transfer* (Oxford University Press, London, 1950).
2. B. C. Wilson and G. Adams, "A Monte Carlo model for the absorption and flux distributions of light in tissue," Med. Phys. **10,** 824–830 (1983).
3. M. Keijzer, S. T. Jacques, S. A. Prahl, and A. J. Welch, "Light distributions in artery tissue: Monte Carlo simulations for finite-diameter laser beams," Lasers Surg. Med. **9,** 148–154 (1989).
4. R. Marchesini, C. Clemente, E. Pignoli, and M. Brambilla, "Optical properties of *in vitro* epidermis and their possible relationship with optical properties of *in vivo* skin," J. Photochem. Photobiol. B **16,** 127–140 (1992).
5. R. Graaff, A. C. M. Dassel, M. H. Koelink, F. F. M. de Mul, J. G. Aarnoudse, and W. G. Zijlstra, "Optical properties of human dermis *in vitro* and *in vivo*," Appl. Opt. **32,** 435–447 (1993).
6. S. L. Jacques, "Time resolved propagation of ultrashort laser pulses within turbid tissues," Appl. Opt. **28,** 2223–2229 (1989).
7. A. Ishimara, "Diffusion of light in turbid material," Appl. Opt. **28,** 2210–2215 (1989).
8. S. Wan, R. R. Anderson, and J. A. Parrish, "Analytical modeling for the optical properties of the skin with *in vitro* and *in vivo* applications," Photochem. Photobiol. **34,** 493–499 (1981).
9. L. G. Henyey and J. L. Greenstein, "Diffuse radiation in the galaxy," Astroph. J. **93,** 70–83 (1941).
10. M. de Belder, J. de Kerf, J. Jespers, and R. Verbrugge, "Light diffusion in photographic layers: its influence on sensitivity and modulation transfer," J. Opt. Soc. Am. **55,** 1261–1268 (1965).
11. M. J. C. van Gemert, S. L. Jacques, H. J. C. M. Sterenborg, and W. M. Star, "Skin optics," IEEE Trans. Biomed. Eng. **36,** 1146–1154 (1989).
12. X. H. Hu, "Efficient use of Q-switched lasers in the treatment of cutaneous lesions," in *Lasers in Surgery: Advanced Characterization, Therapeutics, and Systems* V. R. R. Anderson, ed., Proc. SPIE **2395,** 586–591 (1995).
13. A. H. Hielscher, R. E. Alcouffe, K. M. Hanson, and J. S. George, "Comparison of finite difference transport and diffusion calculations for photon migration in homogeneous and heterogeneous tissues," in *Advances in Optical Imaging and Photon Migration*, R. R. Alfano and J. G. Fujimuto, eds., Vol. 2 of OSA Trends in Optics and Photonics Series (Optical Society of America, Washington, D.C., 1996), pp. 55–59.